Research Article

Chengsheng Li*, Lingwei Kong, Rongjun Shu, Ran An, and Xianwei Zhang

Disintegration characteristics in granite residual soil and their relationship with the collapsing gully in South China

https://doi.org/10.1515/geo-2020-0178
received December 29, 2019; accepted June 18, 2020

Abstract: The climate is a significant factor affecting the collapsing gully in weathered granite areas, and most of the surface layers of the collapsed area comprise granite residual soil. Granite residual soil has complex disintegration characteristics under different initial water content conditions. Besides, its disintegration characteristic is an essential factor for collapsing gully. Therefore, disintegration tests, triaxial shear tests, nuclear magnetic resonance tests, and hydraulic conductivity tests are conducted under torridity and rainstorm conditions in order to study the disintegration characteristics of granite residual soil. The results of disintegration test showed that the initial disintegration rate of granite residual soil increased rapidly with the decrease in water content, while the relationship between disintegration rate and water content in the later stage of disintegration is unclear. When soaked, the maximum decrease in cohesion was 44.48%, the hydraulic conductivity became six times larger, and the amplitude of the T_2 curve increased by about 40%, which reduced the strength of the soil and provided better access for rainwater infiltration to deeper stratum. The results show that the microstructure of granite residual soil would be damaged and the disintegration would occur after a rainstorm at low water content. Micropores would be formed inside the sample after soaking, resulting in destroying the continuity of the material.

*** Corresponding author: Chengsheng Li,** State Key Laboratory of Geomechanics and Geotechnical Engineering, Institute of Rock and Soil Mechanics, Chinese Academy of Sciences, Wuhan, Hubei 430071, China; University of Chinese Academy of Sciences, Beijing 100049, China, e-mail: lichengsheng@outlook.com, tel: + 86 15623646052
Lingwei Kong, Rongjun Shu, Ran An, Xianwei Zhang: State Key Laboratory of Geomechanics and Geotechnical Engineering, Institute of Rock and Soil Mechanics, Chinese Academy of Sciences, Wuhan, Hubei 430071, China; University of Chinese Academy of Sciences, Beijing 100049, China

Keywords: disintegration, granite residual soil, collapsing gully, NMR

1 Introduction

Collapsing gully called *benggang* by local people is a serious soil erosion in the granite-weathered area of southern China; it damages the local landform and even causes disasters [1–3]. After the local surface vegetation damages and suffers from rainstorms, the collapse may occur in the exposed granite-weathered stratum. Collapse disasters frequently occur, however, the mechanism of collapse have not well understood yet. For example, some researchers have investigated the relationship between landform and collapse area [4–7] and performed the slope monitoring or model tests under rainfall conditions [8,9]. Besides, there were some studies on the collapse characteristics and strength characteristics of residual soils [10,11]. However, the analyses of the collapse mechanism are not enough, and the comparative study of the failure mode, strength, and infiltration after soil soaking is not analyzed together. The unsaturated strength characteristics of granite-weathered soils under different initial moisture content conditions have been explored by some researchers [10–12]; nevertheless, the samples were directly tested without the soaking process, that is, the damage caused by rapid infiltration might be ignored.

The surface layer of the mountainous area where the collapse takes place comprise mostly granite residual soil, which is the remnant of weathering granite and retains the characteristics of the original rock structure [13,14]. Granite residual soil has significant anisotropy. There are a large number of initial pores inside the soil, especially after drying, and it is prone to softening and disintegrating after soaking [15,16]. After the rainstorm, the disintegration and destruction of the residual soil layer would be gradually transitioned to deeper weathered stratum, resulting in the formation of a collapsed gully. Therefore, the disintegration and failure characteristics of the granite residual soil are essential.

Granite remnant soil has significant primitive structural characteristics and various initial pores, and good conditions for water infiltration are achieved by the large pores. The hydraulic conductivity coefficient of granite residual soil is between clay and sand. The hydraulic conductivity coefficient would increase after drying, and the pore air pressure would sharply increase during the rapid infiltration [17]. Rapid infiltration would occur in the granite residual soil with low water content at the initial stage of infiltration where the gas in the soil cannot be discharged in time, causing the pore air pressure to rise sharply and then destroy the soil structure. Particularly, the relationship between pore air pressure and soil disintegration was investigated and the effect of initial water content on soil disintegration was analyzed by Cernuda et al. [18]. Besides, the tensile strength of the material is also an important factor affecting the disintegration rate. For instance, the changes in the tensile strength of remolded soils with different water contents before and after soaking were studied by Cernuda et al. [18], revealing that the pore air pressure caused by rapid infiltration could destroy the microstructure of the soil. From a microscopic perspective, Zhang et al. [19] analyzed the forces between two grains and obtained the relationship of the average disintegration rate with the effective porosity and matrix suction; however, the macroscopic mechanical analysis was scarce. Additionally, CT scanning technology was used by Li et al. [20] to study the collapse characteristics of granite residual soil at the initial stage of disintegration, finding that the cracks of the samples were formed significantly. The morphological and evolutionary characteristics of the fissures were quantitatively analyzed while the mechanical analysis was scarce. Generally, these studies lack comparative and relationships among mechanical analysis, microscopic analysis, and undisturbed soils. In most of those studies, the pore air pressure and disintegration tests of materials were only measured while the changes in strength characteristics, microscopic characteristics, and hydraulic conductivity of dry soils after soaking were ignored.

The disintegration of granite residual soil is one of the early stages of collapsing gully. The soil water content may have different states from saturated to unsaturated in a complex climatic environment. Their characteristics, including disintegration rate, strength, and evolution of permeability, are different after soaking. Therefore, the research material selected is undisturbed granite residual soil and the different moisture contents are controlled in a constant temperature–humidity box in order to better understand the disintegration mechanism of the granite residual soil under the complex climate conditions. Then a series of tests, including the disintegration test, consolidated undrained shear test, nuclear magnetic resonance (NMR) test, and hydraulic conductivity test, are separately performed. The disintegration rules of granite residual soil are analyzed from three aspects, that is, disintegration rate, strength characteristics, and micro characteristics.

2 Material and methods

2.1 Material

Granite is the parent rock with the erodibility and the widely distributed area in Guangdong province, China. This type of rock is easily weathered in the humid and hot climate of South China and can form a thick weathering stratum. Granite-weathered stratum is loose and extremely poorly ridged. Hence, it could erode and collapse easily. It is extremely difficult for vegetation to grow. The topsoil would be eroded and exposed to the granite-weathering stratum if the vegetation is damaged, causing strong soil erosion. Strong weathering and gully erosion would occur on granite hillsides with thin weathering stratum, and the clay in weathering stratum is taken away by erosion, leaving coarser grains and highly weathering-resistant quartz particles, leading to rocky desertification. The occurrence of thick granite hillsides would quickly change from surface erosion and gully erosion to landslides. During the rainstorm process, a large amount of quicksand would be the output, the land would be cultivated, silted riverbeds would be threatened, and even local villagers live in danger.

The sample selection site is located at a site in Shenzhen city, Guangdong province, China (22°32′25″E, 113°53′35″N). Because of the heterogeneity of the granite residual soil profile and the mixed soil on the surface, in order to obtain fresh soil samples that are not affected by human or climate, the samples were taken from a foundation pit at depth of 6–8 m with a relatively uniform texture. The local average annual temperature is 22.0°C. The average minimum temperature in January

Figure 1: A typical collapsing gully in the hilly granitic region, consisting of (1) upper catchment, (2) collapsing wall, and (3) colluvial deposit.

is 11.4°C, the average maximum temperature in July is 29.5°C, and the average number of rainy days is 144 days including 9 days of heavy rain and 2.2 days of heavy rainstorm. The amount is 282 mm/day. The maximum value is 385.8 mm/day, and the average precipitation over the years is 1966.5 mm. The rainfall is mainly concentrated in summer. Figure 1 illustrates a typical collapsing gully in an area of Guangdong. It can be divided into three parts, including upper catchment, collapsing wall, and colluvial sediment. Moreover, the surface of the collapsing wall is mostly red granite residual soil. As shown in Figure 2, on the site undisturbed square samples were established to make the test results more reliable. Then the original square samples were wrapped in plastic wrap, foam layer, and wooden boxes. Finally, they were carefully transported to the laboratory. The basic physical parameters of the sample are displayed in Table 1 and Figure 2. It can be seen that the grain size of granite residual soil has a large number of grains and clay, and the hydraulic conductivity coefficient of the soil is relatively large. The soil–water characteristic curve of the drying path was tested by a pressure plate apparatus (see Figure 3(b)).

2.2 Methods

In the natural environment, the weathered soil stratum on the surface is gradually air-dried following which the moisture content reduces and generates cracks. Consequently, it results in collapsing gully after the rainstorm. In this process, in the conversion of saturated to unsaturated soil, the moisture content of the soil changes and finally damaged by rainwater. Therefore, the various characteristics of the granite residual soils after water soaking, including the laws of disintegration, the strength, and hydraulic conductivity evolution of the soil after microstructure damage, need to be further explored in order to achieve a micro perspective analysis of the relationship among them. Previously, most researchers investigated the characteristics of unsaturated strength under different initial water content states [12] while the samples were not soaking in water; thus, the impact of microstructural damage caused by rapid infiltration may be ignored. Therefore, it is necessary to soak samples with different water contents and then simulate the effect of rapid infiltration on the soil at the stage of rainstorm infiltration.

The test steps were designed as:

(1) Cylindrical samples with dimensions of d = 61.8 mm and h = 40 mm were prepared for the disintegration

Figure 2: Photos of specimen: (a) cut soil specimen, and (b) specimen packed in the wooden box.

Table 1: The basic physical properties of granite residue soil

Density ρ (g/cm^3)	Specific gravity G_s	Void ratio e_0	Moisture content (%)	Hydraulic conductivity (m/s)	W_L/%	W_P/%	I_P/%	Grain size (mm/%)				Mineral composition		
								>2	0.075–2	0.005–0.075	<0.005	Quartz	Kaolin	Illite
1.98	2.72	0.74	26.7	1.79×10^{-6}	58.89	27.27	31.61	32.4	20.4	18.1	29.1	71.39	27.10	2.51

test and hydraulic conductivity test. The triaxial samples with dimensions of d = 61.8 mm and h = 120 mm were prepared. The sample was saturated under vacuum pumping to simulate the extreme moisture content of the soil (fully saturated state).

(2) Then the samples were placed in a constant temperature–humidity box. The moisture contents of the samples were controlled as 20.0%, 15.0%, 5.0%, and 0.6%, corresponding to the soil in different moisture content states.

(3) Finally, the samples with different water contents were soaked in water and then the disintegrated test, triaxial shear test, hydraulic conductivity test, and NMR test were performed.

As shown in Figure 4(a), the sample was wrapped with medical gauze in step 3, and the outermost was protected with a porous organic glass tube to prevent the sample from complete disintegration. This was followed by soaking the entire sample in a beaker. The weight of the samples was similar to that of the sample with a moisture content of 20.0% when the sample does not have obvious bubbles after soaking in water in order to avoid the effect of unsaturated effective stress caused by different moisture contents. Moreover, the difference in weight of the samples should be controlled within the range of 5% before performing various tests to more strictly control the difference in moisture content. Meanwhile, the samples with an initial moisture content of 20.0% were not soaked in order to compare the strength evolution of the samples under different initial moisture content disintegration. Simultaneously, the samples after soaking progress were subjected to the NMR and hydraulic conductivity tests to obtain the T_2 distribution curve, NMR imaging diagram, and hydraulic conductivity coefficient of the samples.

The self-made disintegration equipment was employed to perform the disintegration test (Figure 4(b)). The test equipment mainly includes water tank, float, otter board, camera, and stage. Then the disintegration equipment and camera were set up, the water tank was filled with enough water, and the sample was placed on the otter board. Both the sample and the otter board were placed in the water tank for testing. A cross wire mark was attached to the upper end of the float, and the scale change in the float was recorded in real time by the camera because the scale change in the float was relatively small and easy to be affected by floating stains in the later stage of disintegration. Finally, the displacement of the float was accurately measured by the DIC method [21]. The disintegration test was performed with

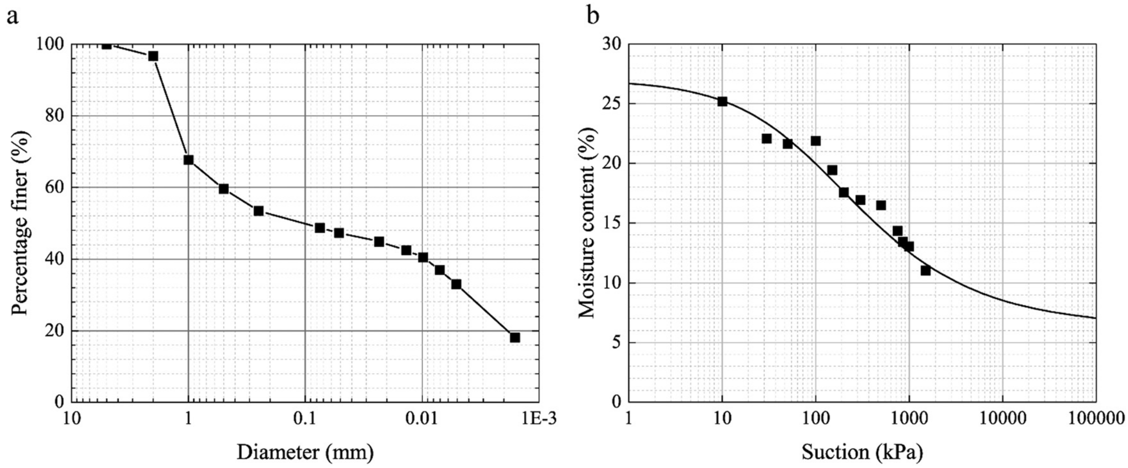

Figure 3: Basic physical properties of material,: (a) grain size distribution, and (b) SWCC curve.

four different water contents in order, and the sample was gradually disintegrated after immersing in water (Figure 4(c)). The real-time disintegration rate is calculated using the following formula:

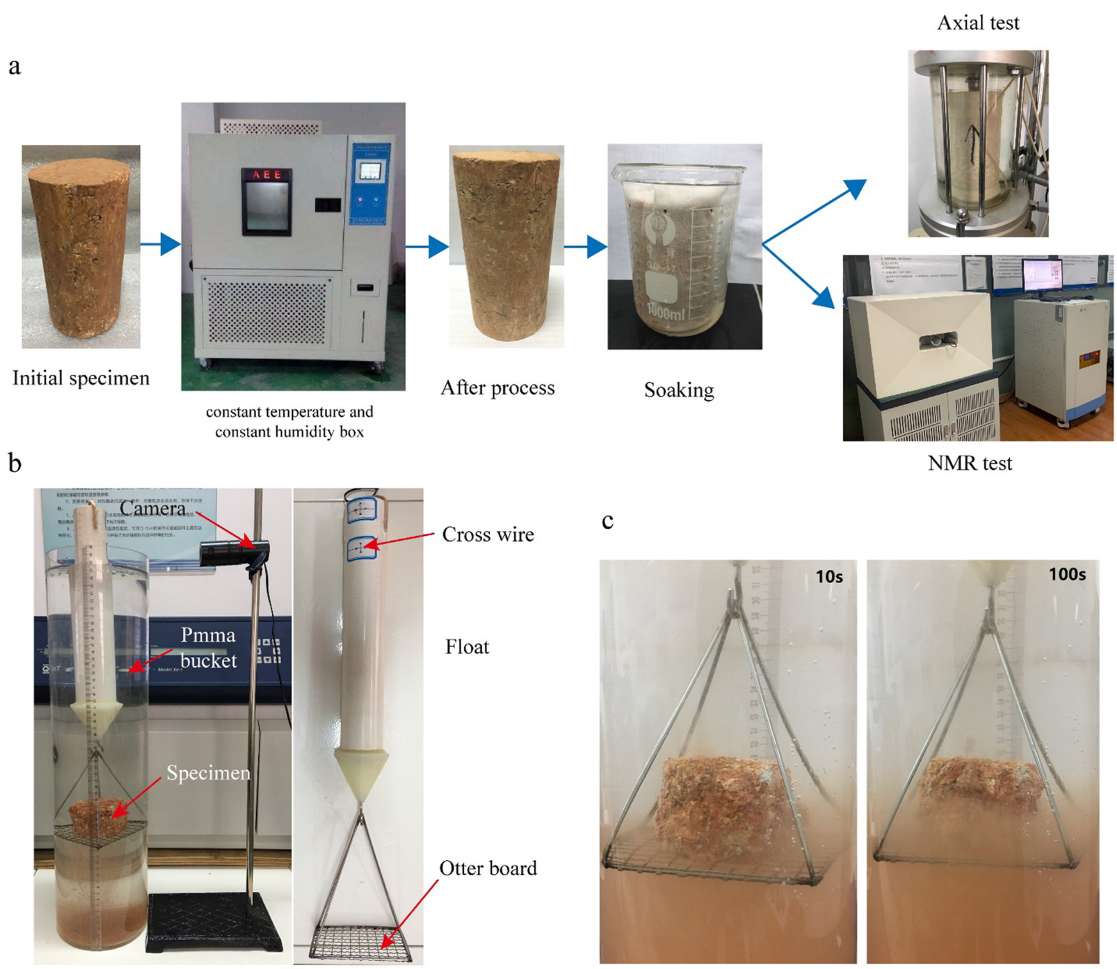

Figure 4: Photographs of disintegration test apparatus: (a) schematic drawing of axial test and NMR test, (b) schematic drawing of self-made disintegration equipment, and (c) photos of the disintegration process.

$$A_t = \frac{m_0 - m_t}{m_0} \times 100\% \quad (1)$$

where m_0 is the initial mass of the sample and m_t is the real-time mass of the sample.

Since bubbles would escape from the sample during the disintegration process, and this part of the pore gas could not be directly measured, which means that the measured disintegration was lower than the actual value, so we referred to the parallel test method [19] and corrected the disintegration results.

In the early stage of disintegration, a large number of bubbles would appear on the surface of the sample. The lower the water content, the more the number of bubbles. In the early stage of the collapse, water rapidly infiltrates into the soil while the gas in the pores could not be discharged in time. With the rapid increase in pore air pressure, the tensile stress in the soil was prone to damage the soil structure, resulting in a decrease in the strength of the soil. In the later stage of collapse, the strength of the surface soil is no longer the main reason, because the sample was close to saturation and became fluid. Therefore, a series of consolidated undrained shear tests, hydraulic conductivity tests, and NMR tests was carried out in order to better understand the mechanical characteristics of granite residual soil in the early stage of disintegration. The constant head hydraulic conductivity tests were carried out under saturated condition.

3 Experimental results and discussion

3.1 Disintegration test results

The disintegration curves and rate curves of different water contents are illustrated in Figure 5. The disintegration curves have "S" characteristics and could be generally divided into two stages. The disintegration curves became steeper and the disintegration rate gradually increased along with the decrease in water content. Especially in the early stage of disintegration, the disintegration rate could reach the maximum value of about 0.45%/s when the moisture content of the sample was 0.6%, the average disintegration rate was less than 0.085%/s and the disintegration rate varied greatly. With the increase in water content, the maximum disintegration rate gradually decreased and the difference among different water contents became smaller; moreover, it was even difficult to classify the disintegration curve. According to the previous analysis, the lower the water content, the higher the water infiltration rate, and the more difficult for the pore gas to be effectively discharged. The larger the pore air pressure in the pores, the more easily the tensile stress would occur in the soil and further damage the soil microstructure; the disintegration rate increased, affecting the strength of the soil. It could be found from the CT disintegration test performed by Li et al. [20] that large penetrating cracks might be caused by the rapid water infiltration, and the hydraulic conductivity of the soil would increase when the moisture content of the granite residual soil was low. Eventually, the water infiltration was accelerated to deeper weathered soil layers, causing further disintegration and destruction.

Many researchers have studied the disintegration mechanism, and the initial disintegration mechanism could be attributed to rapid infiltration. A large number of cracks were generated after the drying of swelling rock. The pore air pressure might increase along with the water infiltration process. Eventually, the material would be broken along the weakest side of the mineral consolidation and gradually disintegrated. Zhang et al. [19] believed that the disintegration of unsaturated granite residual soil was essentially caused by the repulsive force generated by the pore air pressure exceeding the suction between grains. The main reason for the disintegration of unsaturated soil was determined by the matrix suction.

However, it is worth noting that the difference in the disintegration rate of samples with different water content could be ignored in the stage 2 of disintegration, as shown in Figure 5(b). The main reason for this phenomenon was that the moisture content of the sample was close to saturation when the disintegration test was in stage 2. In other words, the difference in moisture content among the samples was not obvious, and the unsaturated stress of the soil was no longer the main influencing factor. Therefore, exploring the characteristics of the early stages of granite residual soil disintegration would be a good method to better understand the mechanism of collapse in the same weathered soil stratum.

3.2 Axial test results

The moisture content of the samples was controlled by the constant temperature and humidity box and then it

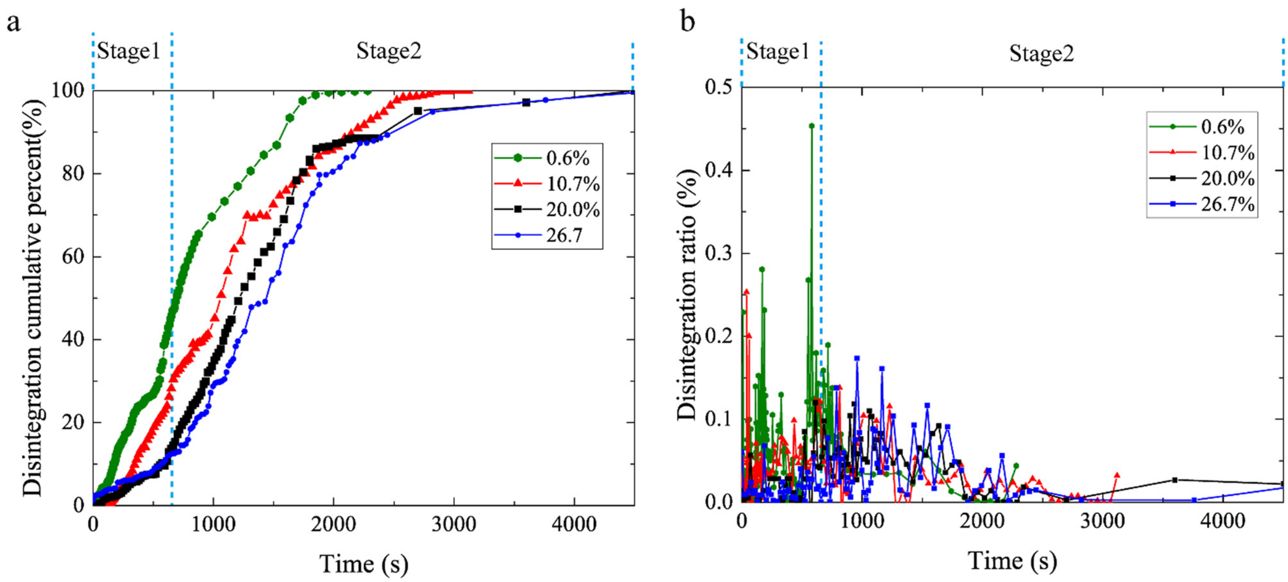

Figure 5: Disintegrating curves of samples: (a) disintegrating curves percent curves, and (b) disintegration rate curves.

was subjected to water immersion treatment. The microstructure of the soil would be destroyed by the rapid water infiltration. The degree of damage varied with the water content. As discussed in the previous section, the lower the moisture content of the sample, the faster the water infiltration rate, and the more significant the microstructure damage caused.

The results of the triaxial shear test stress–strain curves of soaking under different water contents are displayed in Figure 6. Generally, it can be seen that the stiffness and peak strength of the stress–strain curve gradually decreased as the water content decreased. Figure 7 illustrates the strength evolution curve of the disintegrated samples with different initial moisture contents. The cohesion of the soil significantly decreased as the moisture content decreased. The cohesion of the sample decayed from the initial 55.66 to 30.9 kPa, and the percentage of difference was close to 44.48%. In the low water content state, the rate of water infiltration was relatively large. It was difficult for pore gas inside the sample to effectively exhaust. The tensile stress in the material was caused by the rapid rise of pore air pressure. The failure might take place after the tensile stress was larger than the soil strength. Meanwhile, since

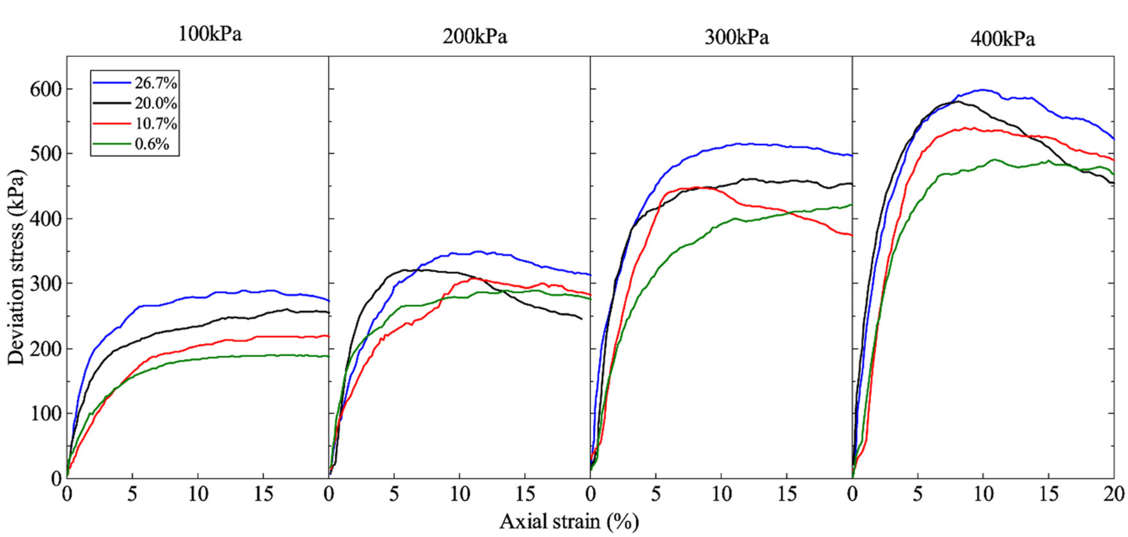

Figure 6: The axial stress–strain curves of different moisture content specimens.

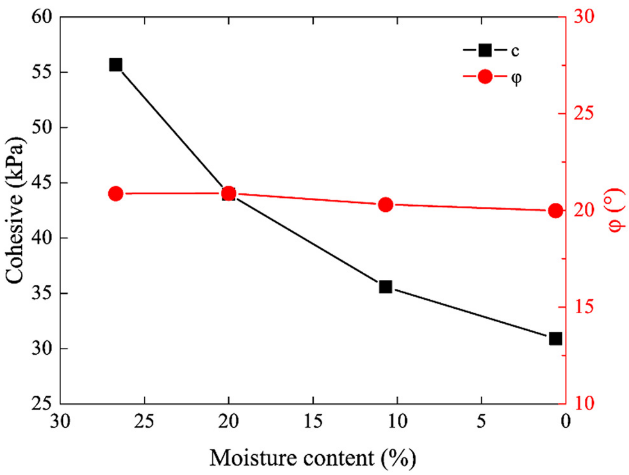

Figure 7: The results of cohesion and φ of different tests.

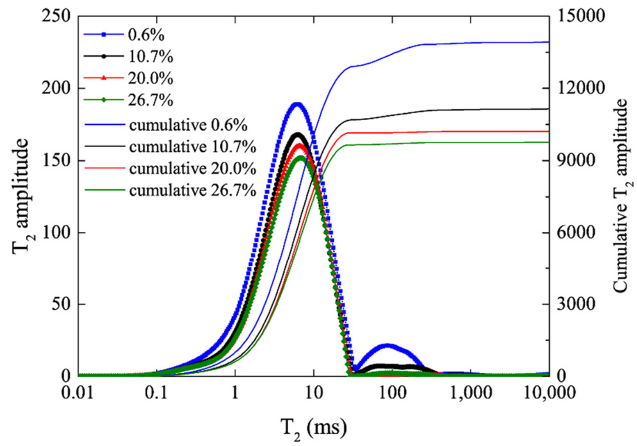

Figure 8: T_2 amplitude and cumulative of different moisture content specimens.

the water immersion of the sample is difficult to affect the coarse grain structure inside the sample and the friction angle is also less affected, the infiltrating water would cause damage to the soil near the seepage path. The larger the infiltration rate, the larger the damage. However, the change in the friction angle of the soil was small.

Cohesion is an important factor of disintegration resistance [6], and cohesion is positively related to the tensile strength [22]. The characteristics of the tensile strength of the remolded granite residual soil with different water contents, and different chemical solutions were investigated by Tang et al. [22,23], concluding that the tensile strength of the remolded granite residual soil was between 5 and 20 kPa. According to the collapse model test [9], it is known that cracks are easily generated on the backside of the slope. The decrease in cohesion would cause the tensile strength of the soil to decrease. The stability of the slope behind the collapsed surface becomes worse. With the further development of water infiltration and collapse, larger scale collapse disasters would gradually occur.

3.3 NMR test results

The T_2 distribution of samples with different initial moisture contents after soaking treatment is illustrated in Figure 8. Generally, the amplitude of the T_2 curve gradually increased as the water content decreased. It increased to the largest when the moisture content was 0.6%, increment was nearly 40%. In the range of [0.1, 30 ms], the T_2 amplitude of low water content is generally larger than that of the large water content, even in the range of [0.1, 1 ms]. This phenomenon indicated that the pore air pressure would destroy the microstructure and increase the micropore content during the rapid infiltration of water. In the range of [30, 1,000 ms], the difference in T_2 results among the different moisture contents was more significant, and the T_2 amplitude increased sharply when the moisture content was 0.6%. This phenomenon indicated that the rate of water infiltration was faster and the pore air pressure inside the sample could be larger under the condition of low water content. This could generate both micropores and larger sized pores. The internal continuity of the sample was destroyed as the macropore content increased, affecting the strength of the material. This provided better percolation channels and accelerated the rate of water infiltration and disintegration.

The internal pore content of the material was indirectly reflected by the cumulative T_2 amplitude. The relationship among cohesion, hydraulic conductivity coefficient, and cumulative T_2 amplitude is shown in Figure 9. It can be seen that the cohesive force and the cumulative T_2 amplitude value were inversely proportional to the decaying relationship while the hydraulic conductivity coefficient and the cumulative T_2 amplitude value were proportionally increasing. With the increase in cumulative T_2 amplitude, the cohesive force gradually decreased and the rate of decrease gradually decreased. The decay rate of the curve indicated that the sensitivity of the material cohesion to the change in the pore content was different. The cohesion of the material rapidly decreased when the pore content of the sample increased. Meanwhile, the change in cohesion was not so significant as the pore content continued to increase. The hydraulic conductivity coefficient increased as the

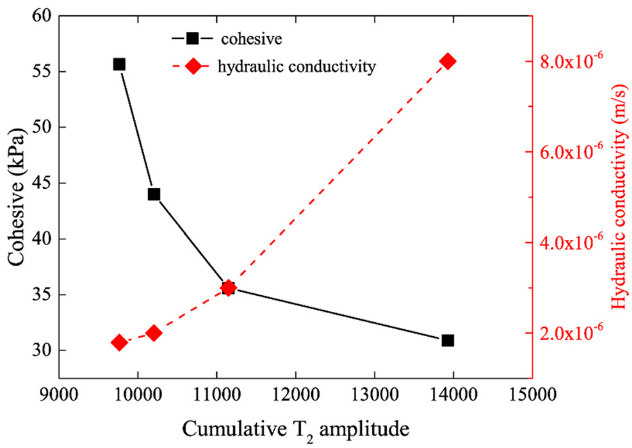

Figure 9: The relationship between cohesive and hydraulic conductivity with cumulative T_2 amplitude.

cumulative T_2 amplitude value increased, and the growth rate gradually increased. Especially, the hydraulic conductivity coefficient increases nearly six times when the water content was 0.6%, which provided better conditions for later water infiltration and accelerated disintegration or collapse.

The NMR imaging test was performed at the same time after the samples were soaked in water. Three cross-sections parallel to the z-axis of the sample were selected as the imaging plane, and they could better reflect the overall characteristics of the material. As demonstrated in Figure 10, the brightly colored area represented the location of water molecules and the dark blue area was the background color. The brighter the color, the higher the water content, thereby indicating that the pore size was generally larger.

The water existed in the initial pores of the material, and its distribution was anisotropy when the water content was 26.7%. The area of the color highlight area gradually increased as the moisture content decreased. The lower the water content, the larger the water infiltration rate and the larger the pore air pressure. The generated tensile stress exceeds the strength of the material and might destroy the microstructure. The pore content, pore size, and the area of the corresponding bright color increased. It was worth noting in Figure 10 that water gradually infiltrates from the surface of the sample to the inside during the water soaking process; therefore, the surface layer of the sample was more prone to large pores or cracks. The most significant result was a moisture content of 0.6%. Particularly, the effect of pore hydraulic conductivity was most significant when the moisture content was 0.6%. The results demonstrated the presence of large pores or cracks, which is similar to the conclusion of the disintegration CT test performed by Li et al. [20].

Based on the above test results, the pore pressure caused by transient infiltration could not be ignored when granite residual soil is at the state of low water content. When the water content was less than 10%, the pore pressure caused by rapid infiltration during disintegration process may cause collapse failure of granite residual soil.

4 Conclusions

In this study, the disintegration characteristics of granite residual soil and its strength, hydraulic conductivity, and microscopic characteristics after soaking have been studied, and the disintegration or collapse mechanism has been revealed from multiple angles:

(1) The disintegration test reveals that in the early stage of disintegration, the disintegration rate of the granite residual soil gradually increases as the water content decreases. In the second stage of disintegration, the difference in disintegration rates with different water contents could be ignored. The unsaturated effective stress is no longer the main influencing factor. The microstructure of the soil would be destroyed by the pore air pressure after soaking. With the decrease in water content, the cohesion and hydraulic conductivity coefficients decrease and increase, respectively; however, the correlation between the internal friction angle and the water content is low.

(2) The NMR test results illustrate that the pore content of the sample increases as the water content after soaking decreases. There is a tendency to penetrate from the outside to the inside. With the increase in pore content, cohesion and hydraulic conductivity coefficients decrease and increase, respectively. After the increase in hydraulic conductivity coefficient, water could rapidly infiltrate into the soil and continue to destroy the continuity and strength of the soil, resulting in increasing the probability of subsequent disintegration and damage and also facilitating the infiltration of water into deeper weathered stratum.

(3) The two main reasons for the disintegration of granite residual soil are listed as follows. First, the moisture content of the granite residual soil is reduced and cracks are formed after exposure to air. Second, the infiltration water source is provided

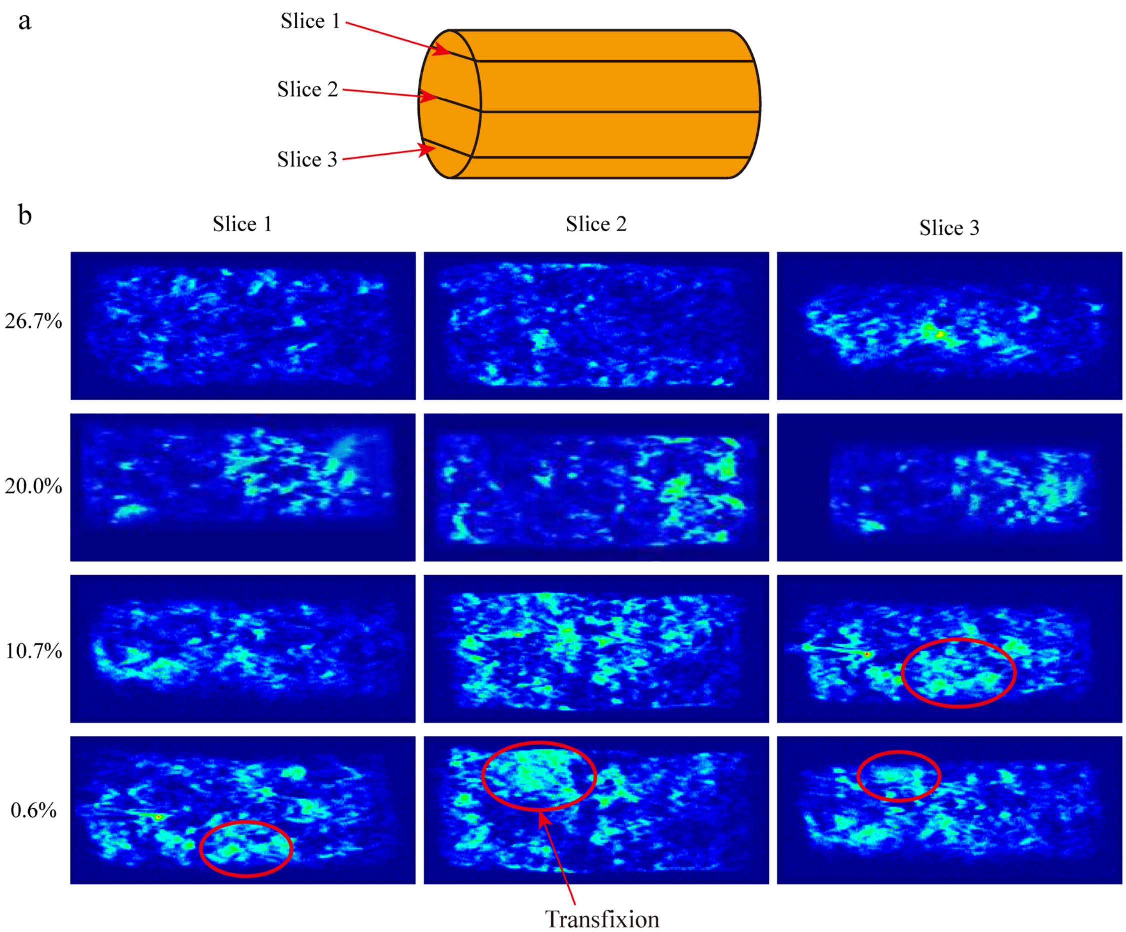

Figure 10: The NMR images results: (a) schematic diagram of MRI section of the sample, (b) the NMR images of different moisture content specimens.

by the rainstorm. The two factors are indispensable. Therefore, those two factors need to be considered in the governance of collapses; for example, the vegetation in the weathered soil layer should be protected in order to retain the moisture content of the surface residual soil and control the formation of cracks. Then it is required to control the surface water source and add some drainage channels.

(4) In the granite residual soil area, if the slope is excavated or the vegetation is damaged and the slope surface is exposed, this will increase the erosion effects of water and gravity. The disintegration of granite residual soil reduces the strength and increases the permeability of the soil. At the same time, the disintegration of the soil provides a source of material for erosion. The collapsed landform eventually forms.

Acknowledgments: This work is supported by the National Natural Science Foundation of China (Grant nos. 11672320 and 41372314).

Authors contribution: Chengsheng Li: Methodology, Test, Validation, Writing. Lingwei Kong: Conceptualization, Reviewing. Rongjun Shu: Writing, Reviewing and Editing. Ran An: Reviewing and Editing. Xianwei Zhang: Reviewing and Editing.

References

[1] Luk SH, diCenzo PD, Liu XZ. Water and sediment yield from a small catchment in the hilly granitic region, South China. Catena. 1997;29:177–89. doi: 10.1016/s0341-8162(96)00054-9.

[2] Liu XL, Qiu JN, Zhang DL. Characteristics of slope runoff and soil water content in benggang colluvium under simulated rainfall. J Soils Sedim. 2018;18:39–48. doi: 10.1007/s11368-017-1742-0.

[3] Xu JX. Benggang erosion: the influencing factors. Catena. 1996;27:249–63. doi: 10.1016/0341-8162(96)00014-8.

[4] Ji X, Thompson A, Lin JS, Jiang FS, Li SX, Yu MM, et al. Simulating and assessing the evolution of collapsing gullies based on cellular automata-Markov and landscape pattern metrics: a case study in Southern China. J Soils Sedim. 2019;19:3044–55. doi: 10.1007/s11368-019-02281-y.

[5] Liao YS, Yuan ZJ, Zheng MG, Li DQ, Nie XD, Wu XL, et al. The spatial distribution of Benngang and the factors that influence it. Land Degrad Dev. 2019;30(18):2323–35. doi: 10.1002/ldr.3418.
[6] Wang JG, Feng SY, Ni SM, Wen H, Cai CF, Guo ZL. Soil detachment by overland flow on hillslopes with permanent gullies in the Granite area of southeast China. Catena. 2019;183:104235. doi: 10.1016/j.catena.2019.104235.
[7] Wang C, Ross GJ, Rees HW. Characteristics of residual and colluvial soils developed on granite and of the associated pre-Wisconsin landforms in north-central New Brunswick. Canadian J Earth Sci. 1981;18:487–94. doi: 10.1139/e81-042.
[8] Tao Y, He YB, Duan XQ, Zou ZQ, Lin LR, Chen JZ. Preferential flows and soil moistures on a Benggang slope: Determined by the water and temperature co-monitoring. J Hydrol. 2017;553:678–90. doi: 10.1016/j.jhydrol.2017.08.029.
[9] Liu WP, Song XQ, Luo J, Hu LN. The processes and mechanisms of collapsing erosion for granite residual soil in southern China. J Soils Sedim. 2019;20:992–1002. doi: 10.1007/s11368-019-02467-4.
[10] Deng YS, Duan XQ, Ding SW, Cai CF, Chen JZ. Suction stress characteristics in granite red soils and their relationship with the collapsing gully in south China. Catena. 2018;171:505–22. doi: 10.1016/j.catena.2018.07.043.
[11] Xia JW, Cai CF, Wei YJ, Wu XL. Granite residual soil properties in collapsing gullies of south China: spatial variations and effects on collapsing gully erosion. Catena. 2019;174:469–77. doi: 10.1016/j.catena.2018.11.015.
[12] Zhang XM, Ding SW, Cai CF. Effects of drying and wetting on nonlinear decay of soil shear strength in slope disintegration erosion area. Trans Chinese Soc Agric Eng. 2012;28:241–5. doi: 10.3969/j.issn.1002-6819.2012.05.040.
[13] Kajdas BO, Michalik MJ, Migoń P. Mechanisms of granite alteration into grus, Karkonosze granite, SW Poland. Catena. 2017;150:230–45. doi: 10.1016/j.catena.2016.11.026.
[14] Padrones JT, Imai A, Takahashi R. Geochemical Behavior of Rare Earth Elements in Weathered Granitic Rocks in Northern Palawan, Philippines. Resource Geol. 2017;67(3):231–53. doi: 10.1111/rge.12123.
[15] Luk SH, Yao QY, Gao JQ, Zhang JQ, He YG, Huang SM. Environmental analysis of soil erosion in Guangdong Province: a Deqing case study. Catena. 1997;29:97–113. doi: 10.1016/s0341-8162(96)00049-5.
[16] Shen P, Zhang LM, Chen HX, Gao L. Role of vegetation restoration in mitigating hillslope erosion and debris flows. Eng Geol. 2016;216(12):122–33. doi: 10.1016/j.enggeo.2016.11.019.
[17] Collis-George N, Bond WJ. Ponded infiltration into simple soil systems: 2. Pore air pressures ahead of and behind the wetting front. Soil Sci. 1981;131:263–70. doi: 10.1097/00010694-198104000-00002.
[18] Cernuda CF, Smith RM, Vicente-Chandler J. Influence of initial soil moisture condition on resistance of macroaggregates to slaking and water-drop impact. Soil Sci. 1954;77(1):19–28. doi: 10.1097/00010694-195401000-00003.
[19] Zhang S, Tang HM. Experimental study of disintegration mechanism for unsaturated granite residual soil. Rock Soil Mech. 2013;34:1668–74. doi: CNKI:SUN:YTLX.0.2013-06-023.
[20] Li CS, Kong LW, Guo AG, Zhang XW. X-ray microscopic study on disintegration of granite residual soil. 7th International Symposium on Deformation Characteristics of Geomaterials, IS-Glasgow 2019, June 26, 2019–June 28, 2019. 2019, Glasgow, United kingdom: EDP Sciences. doi: 10.1051/e3sconf/20199209006.
[21] Pan B, Li K, Tong W. Fast, robust and accurate digital image correlation calculation without redundant computations. Exp Mech. 2013;53:1277–89. doi: 10.1007/s11340-013-9717-6.
[22] Tang LS, Sang HT, Hou T, Song J, Chen HK, et al. Experimental study on tensile strength of granite residual soil. Acta Sci Nat Univ Sunyatsni. 2014;53:98–105.
[23] Sun YL, Tang LS. The effect of chemical composition on tensile mechanics of residual granite soils. Acta Sci Nat Univ Sunyatseni. 2018;57:7–13.